Original Article

The diagnostic value of MRI for architectural distortion categorized as BI-RADS category 3–4 by mammography

Haibing Mei[1], Jian Xu[1], Gang Yao[2]^, Ying Wang[1]

[1]Department of Radiology, Ningbo Women & Children's Hospital, Ningbo, China; [2]Department of Radiology, Sir Run Run Hospital, Nanjing Medical University, Nanjing, China

Contributions: (I) Conception and design: H Mei, J Xu, G Yao; (II) Administrative support: H Mei, G Yao; (III) Provision of study materials or patients: J Xu, Y Wang; (IV) Collection and assembly of data: H Mei, J Xu, Y Wang; (V) Data analysis and interpretation: J Xu, G Yao, Y Wang; (VI) Manuscript writing: All authors; (VII) Final approval of manuscript: All authors.

Correspondence to: Gang Yao. Department of Radiology, Sir Run Run Hospital, Nanjing Medical University, Nanjing 211166, China.
Email: yaogang0303@aliyun.com.

Background: Architectural distortion is a common mammographic sign that can be benign or malignant. This study investigated the diagnostic value of magnetic resonance imaging (MRI) for architectural distortions that were category 3–4 under the breast imaging reporting and data system (BI-RADS) by mammography.

Methods: We retrospectively analyzed 219 pathologically confirmed lesions in 208 patients who had BI-RADS category 3–4 architectural distortion in mammography images. Two radiologists described and categorized the architectural distortion and assigned the BI-RADS categories to the corresponding lesions on MRI images. Using the postoperative pathological diagnosis as the gold standard, we performed receiver operating characteristic (ROC) analysis for the efficacy of mammography and MRI in differentiating patients with benign or malignant lesions.

Results: Totally 151 benign lesions and 68 malignant lesions were confirmed. According to the full-field digital mammography (FFDM), 82 lesions were in BI-RADS category 3, 104 lesions in 4A, 29 lesions in 4B, and 4 lesions in 4C. The positive predictive values of FFDM for BI-RADS categories 3, 4A, 4B, and 4C were 13.4% (11/82), 27.9% (29/104), 82.8% (24/29), and 100.0% (4/4), respectively. According to MRI, 59 lesions were in BI-RADS categories 1–2, 87 lesions in 3, 39 lesions in 4, and 34 lesions in 5, with their positive predictive values being 0.0% (0/58), 2.3% (2/87), 89.7% (35/39), and 100.0% (34/34), respectively. The area under the ROC curve (AUC) of breast benign and malignant lesions differentiated by FFDM was 0.647, and the diagnostic sensitivity, specificity, and Youden index were 86.3%, 41.7%, and 0.280, respectively. The AUC of FFDM combined with dynamic contrast-enhanced MRI (DCE-MRI) in differentiating breast benign *vs.* malignant lesions was 0.851, and the diagnostic sensitivity, specificity, and Youden index were 89.2%, 80.7%, and 0.699, respectively. The AUC of FFDM combined with DCE-MRI and the apparent diffusion coefficient (ADC) in differentiating benign *vs.* malignant lesions was 0.983, and the diagnostic sensitivity, specificity, and Youden index were 98.1%, 97.5%, and 0.956, respectively.

Conclusions: MRI can improve the diagnostic efficiency of mammography in diagnosing BI-RADS category 3–4 architectural distortions and can help in the qualitative diagnosis of architectural distortion lesions.

Keywords: Mammography; magnetic resonance imaging (MRI); architectural distortion

Submitted Mar 30, 2020. Accepted for publication Jul 08, 2020.
doi: 10.21037/gs-20-505
View this article at: http://dx.doi.org/10.21037/gs-20-505

^ ORCID: 0000-0001-5890-2056.

Introduction

Breast imaging reporting and data system (BI-RADS) is a scoring system that was used to describe mammogram results (1). The categories are from 0 to 6. The description of BI-RADS in full-field digital mammography (FFDM) including mass, calcification, architectural distortion, asymmetry, and accompanying signs (2). It can help identify anything abnormal but cannot medically diagnose breast carcinoma, since not all abnormal findings are considered cancerous. The treatment of breast carcinoma includes surgical treatment, chemotherapy, radiotherapy, endocrine therapy, and individualized treatments. The individualized treatment of breast carcinoma is currently the most effective, less invasive and economical treatment. However, accurate imaging diagnosis is the key of the individualized treatment.

Architectural distortion is defined as an architectural disruption of the normal breast that does not have obvious mass opacities, which may be early signs of breast carcinoma (3). Primary architectural distortion of the breast refers to the distortion except for those caused by postoperative breast changes, infections, or trauma in FFDM. FFDM is highly sensitive in detecting the architectural distortion. BI-RADS category 3–4 architectural distortion lesions can be benign or malignant, which reduces the diagnostic specificity of FFDM. Biopsy is needed when the description is BI-RADS category 4 in FFDM but it is an invasive examination. A noninvasive examination that can diagnose this type of lesion in clinical practice is needed.

Currently, some researches investigated the imaging characteristics of architectural distortion combined with calcification or mass, and obtained accurate diagnosis results since calcification or mass is a typical sign to diagnose tumor malignancy (4). However, the simple architectural distortion is easy to misdiagnosis in FFDM, and magnetic resonance imaging (MRI) is more valuable for the diagnosis of such diseases. The aim of this study is to investigate the diagnostic value of adding MRI to FFDM for BI-RADS category 3–4 architectural distortions by analyzing the morphological characteristics on MRI in order to improve the diagnostic efficiency for patients with such lesions. We present the following article in accordance with the STROBE reporting checklist (available at http://dx.doi.org/10.21037/gs-20-505).

Methods

Subjects

This study retrospectively analyzed patients in our hospital between March 2016 and February 2020 who met the following criteria. Inclusion criteria: (I) patients with BI-RADS category 3–4 local architectural distortion not accompanied by calcification or mass as determined by two radiologists on the FFDM; (II) patients with or without asymmetric density; (III) patients who underwent breast MRI planar scanning and enhanced examination within 2 months after FFDM (non-menopausal women underwent breast examination 3–7 days after menstruation); (IV) patients who did not undergo radiotherapy, chemotherapy, biopsy, or surgery; and (V) patients whose diagnosis was confirmed by biopsy or surgical pathology. Exclusion criteria: (I) patients with BI-RADS category 1, 2, or 5 lesions on FFDM; and (II) patients whose imaging quality was too poor to be used for analysis. A total of 208 patients with 219 lesions were included in the study. All the patients were females aged 17–76 years (average age 45.56±9.78 years). This study was approved by the Ethics Committee of Ningbo Women & Children's Hospital (Approval No: EC2020-023). The study was conducted in accordance with the Declaration of Helsinki (as revised in 2003). Written informed consent was obtained from all patients.

Imaging methods

FFDM

Patients underwent mammographic examination with the routine craniocaudal view and mediolateral oblique view using the Senographe DS full-field digital mammography (GE, USA) equipped with a three-dimensional wire positioning device and biopsy system.

MRI examination

MRI was performed on the Philips Achieva Noval Dual 1.5-T superconducting dual-gradient MRI scanner using the eight-channel coil specialized for breast examination. Cross-sectional turbo spin-echo T2-weighted image (T2WI) sequences were acquired using the spectrally selective attenuated inversion recovery fat suppression technique with repetition time (TR) 4,000 ms, echo time (TE) 70 ms, layer thickness 3.0 mm, layer interval 3 mm, and field

of view (FOV) 360 mm × 360 mm. Diffusion-weighted imaging (DWI) was acquired using the axial single-shot echo-planar imaging technique with TR 11,700 ms, TE 73 ms, layer thickness 3 mm, layer interval 3 mm, and b= 0, 800 s mm^{-2}, and the apparent diffusion coefficient (ADC) was generated automatically by the post-processing software. Dynamic contrast-enhanced (DCE) MRI used axial fat suppression T1 high-resolution isotropic volume excitation (THRIVE) to generate three-dimensional imaging T1WI sequences with TR 6.91 ms, TE 3.39 ms, layer thickness 2.5 mm, and layer interval 1.3 mm. A total of six phases were repeatedly scanned, and each scan took approximately 65 s. After completing the scanning of the first phase, the contrast agent gadolinium-diethylenetriamine pentaacetic acid was injected into the cubital vein with a high-pressure syringe at a dose of 0.2 mmol/kg (15–20 mL) and an injection flow rate of 2.50 mL/s.

Image analysis

Two highly experienced radiologists described and classified the architectural distortion in mammographs according to the 2013 BI-RADS classification criteria of the American College of Radiology and assigned the BI-RADS categories to the corresponding lesions on MR images. The mammographic and MR images of all patients were stored in the picture archiving and communication systems (PACS) format. The above two radiologists analyzed the MRI images together by referring to the architectural distortion in FFDM without knowing the pathology, ensured that the included lesions matched the MRI lesions, and assigned MRI BI-RADS classification to the lesions.

Statistical analysis

Data were analyzed using SPSS 25.0 and MedCalc 19.0.7 software. The Kolmogorov-Smirnov test was performed to determine whether quantitative data conformed to the normal distribution. Data with a normal distribution were represented by $\bar{x} \pm s$. The χ^2 test was performed on the data of the morphology, distribution, and pathology of the architectural distortion lesions in mammographic images. The differences in the ADC values between patients with benign and malignant lesions were determined by the independent-sample *t* test. The diagnostic efficiency of mammography was subjected to receiver operating characteristic (ROC) analysis using postoperative pathological diagnosis as the gold standard, with malignant tumors being positive and benign lesions being negative. The ROC curves of mammography, MRI, and mammography + MRI were plotted to analyze their diagnostic performance, and the area under curve (AUC), sensitivity, specificity, and Youden index of the two diagnostic methods were calculated. Differences with P<0.05 were considered statistically significant.

Results

Pathological results

A total of 219 lesions were included in the study. One hundred fifty-one lesions were benign and 68 lesions were malignant. The detailed pathological results of included lesions are shown in *Table 1*.

FFDM manifestations

Among the 219 lesions, 82 were in BI-RADS category 3, 104 were in category 4A, 29 were in category 4B, and 4 were in category 4C. The positive predictive values of FFDM for BI-RADS categories 3, 4A, 4B and 4C were 13.4% (11/82), 27.9% (29/104), 82.8% (24/29), and 100.0% (4/4), respectively. The differences between benign and malignant architectural distortion and/or asymmetric-density lesions were significant (P<0.05) (*Table 2*).

MRI manifestations

According to MRI-BI-RADS, 59 out of the 219 lesions were in categories 1–2, 87 were in category 3, 39 were in category 4, and 34 were in category 5. Their positive predictive values of MRI for these categories were 0.0% (0/59), 2.3% (2/87), 89.7% (35/39), and 100.0% (34/34), respectively. Among the 151 benign lesions, the MRI-enhanced morphological manifestations were as follows: seven lesions showed no enhancement, 76 lesions showed mass-like enhancement, and 42 lesions showed non-mass-like enhancement. Among the 68 malignant lesions, 44 lesions showed mass-like enhancement, and 24 lesions showed non-mass-like enhancement. The differences in the MRI enhancement types and time-intensity curve (TIC) types were significantly different between patients with benign and malignant lesions (P<0.05). The differences in internal enhancement characteristics,

Table 1 Pathological results of included lesions

Lesions (n=219)	Category	Number
Benign lesions (n=151)	Breast adenopathy	73
	Breast fibroadenoma	48
	Intraductal papilloma	12
	Breast inflammation	8
	Fibrocystic disease	7
	Benign phyllodes tumor	2
	Hamartoma	1
Malignant lesions (n=68)	Invasive ductal carcinoma	54
	Ductal carcinoma *in situ*	7
	Invasive lobular carcinoma	4
	Borderline phyllodes tumor	2
	Intraductal papillary carcinoma	1

Table 2 Mammographic manifestations of architectural distortion accompanied or not by asymmetric density and the enhancement characteristics of the benign and malignant lesions on DCE-MRI

Indicators	Benign	Malignant	χ^2 value	P value
Lesion number	151	68	–	–
Mammographic manifestation			13.996	0.001 (P<0.05)
Architectural distortion	73	15		
Asymmetric density	50	37		
Architectural distortion lesions accompanied with asymmetric density	28	16		
MRI enhancement type			40.612	0.000 (P<0.05)
Dot-like	26	0		
Mass-like	76	44		
Non-mass such as	42	24		
No enhancement	7	0		
TIC curve type*			98.852	0.000 (P<0.05)
Ascending	87	2		
Platform	47	21		
Outflowing	10	45		

*, seven breast benign lesions did not show enhancement, so they did not have a TIC (totally 144 benign lesions). DCE-MRI, dynamic contrast-enhanced MRI; TIC, time-intensity curve.

enhancement morphology, and enhancement edges of the MRI mass-like enhancement between the benign and malignant lesions were significant (P<0.05) (*Table 3*). The MRI non-mass-like enhancement had significantly different distribution characteristics and internal enhancement features between benign and malignant lesions (*Table 4*). The malignant lesions on DWI showed a high signal of diffusion limitation, and the ADC values

Table 3 The DCE-MRI characteristics of benign and malignant lesions with local architectural distortion that were manifested as mass-like enhancements

Indicators	Benign	Malignant	χ^2 value	P value
Case number	76	44	–	–
Internal enhancement characteristics			51.617	0.000 (P<0.05)
Even	38	0		
Uneven	16	34		
Annulus	10	10		
No enhancement in the internal division	12	0		
Morphology			38.461	0.000 (P<0.05)
Circular or lobulated	55	6		
Irregular	21	38		
Borderline			40.672	0.000 (P<0.05)
Clear	66	13		
Not clear	10	31		

DCE-MRI, dynamic contrast-enhanced MRI.

Table 4 The DCE-MRI characteristics of benign and malignant lesions with local architectural distortion that were manifested as non-mass-like enhancements

Indicators	Benign	Malignant	χ^2 value	P value
Case number	42	24	–	–
Distribution characteristics			12.101	0.017 (P<0.05)
Speckled	10	0		
Linear	3	3		
Segmental	13	16		
Regional	12	4		
Multiregional	4	1		
Internal enhancement			17.909	0.000 (P<0.05)
Even	25	3		
Uneven	7	13		
Clustered	4	6		
Ring clustered	6	2		

DCE-MRI, dynamic contrast-enhanced MRI.

of benign and malignant lesions were (1.72±0.29)×10^{-3} mm^2/s and (1.02±0.31)×10^{-3} mm^2/s, respectively (P<0.05). Among patients with pathologically confirmed breast cancer, the classification of the mammography of 41 malignant lesions was raised to 4 to 5 after MRI (typical images shown in *Figure 1*). Among the patients with pathologically confirmed benign lesions, the categories of 79 lesions in mammography BI-RADS category 4 were reduced to categories 2–3 after MRI examination (representative examples shown in *Figure 2*).

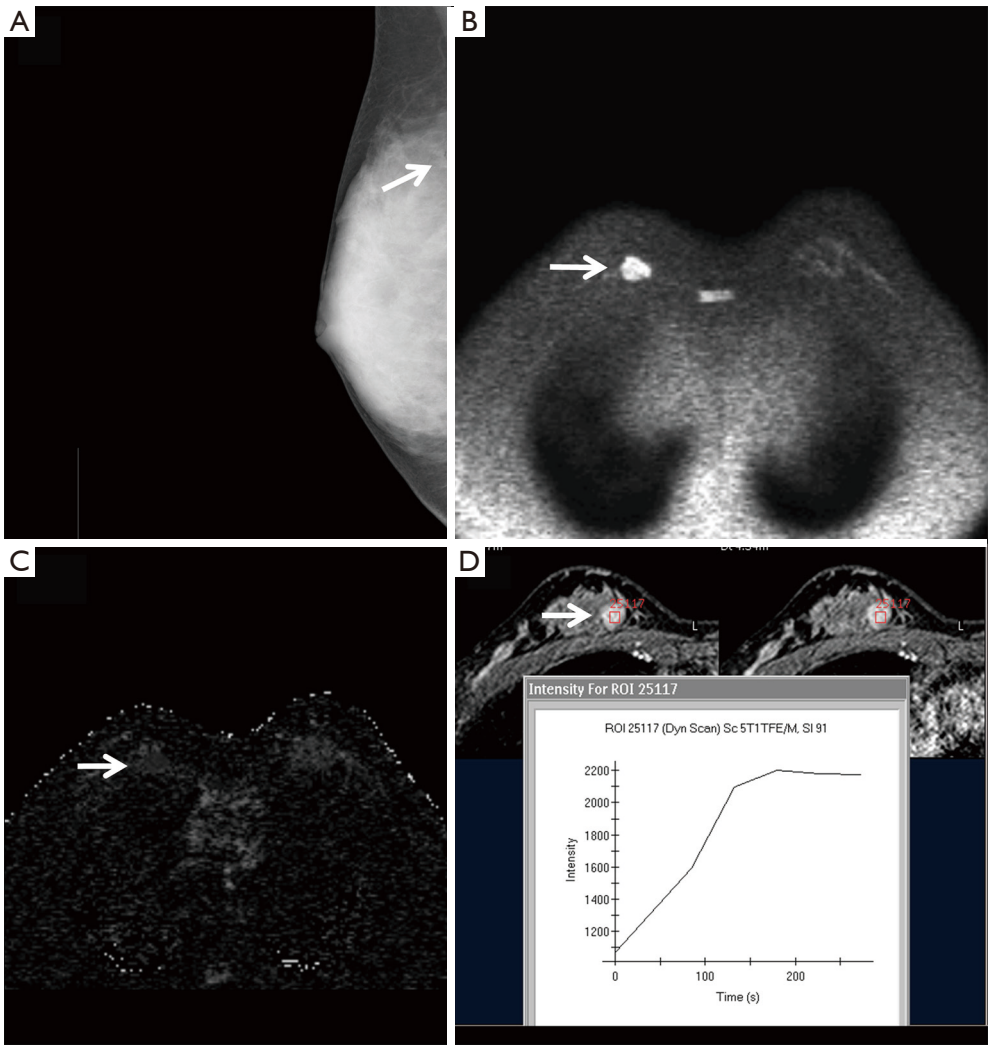

Figure 1 A 34-year-old female patient with right breast invasive ductal carcinoma. (A) Craniocaudal view of the FFDM with an architectural distortion in the inner upper region of the right breast that was in BI-RADS category 3 by mammography (arrow); (B) MRI diffuse axial view with a nodular DWI high-signal-intensity opacity in the inner upper region of the right breast (arrow); (C) MRI diffuse axial view, with the lesion ADC showing a significantly low signal (arrow); (D) significant enhancement of the lesion, with the TIC curve being flat. FFDM, full-field digital mammography; BI-RADS, breast imaging reporting and data system; TIC, time-intensity curve.

Diagnostic efficiency

The BI-RADS classification results of the local architectural distortion by FFDM, FFDM + DCE-MRI, and FFDM + DCE-MRI + ADC are shown in *Table 5* and *Figure 3*. Statistical analysis showed that the AUC of FFDM in differentiating benign *vs.* malignant breast lesions was 0.647 [95% confidence interval (CI): 0.556–0.719], and the diagnostic sensitivity, specificity, and Youden index were 86.3%, 41.7%, and 0.280, respectively. The AUC of FFDM + DCE-MRI in differentiating benign *vs.* malignant lesions was 0.851 (95% CI: 0.793–0.913), and the diagnostic sensitivity, specificity, and Youden index were 89.2%, 80.7%, and 0.699, respectively. The AUC of FFDM + DCE-MRI + ADC in differentiating benign *vs.* malignant lesions was 0.983 (95% CI: 0.956–0.999), and the diagnostic sensitivity, specificity, and Youden index were 98.1%, 97.5%, and 0.956, respectively.

Discussion

The common causes of architectural distortion include local

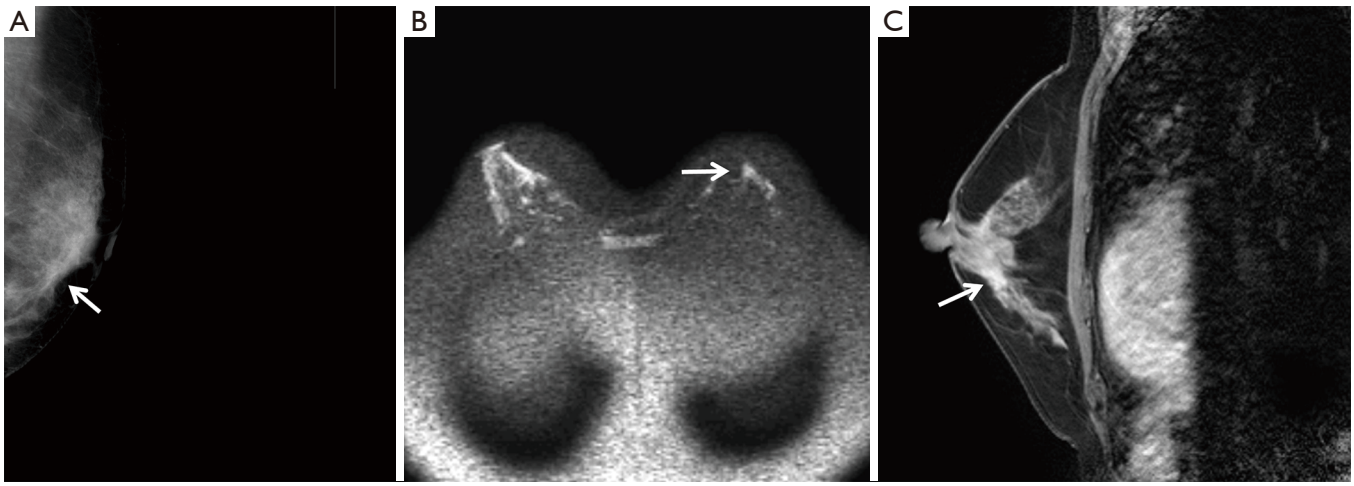

Figure 2 A 46-year-old female patient with left breast adenosis. (A) Craniocaudal view of the FFDM with an architectural distortion in the slightly lower region of the left breast that was in BI-RADS category 3 (arrow); (B) on the MRI diffuse axial view, DWI showed a slightly highly striped signal (arrow); (C) on the MRI enhanced oblique sagittal view, the lesion was enhanced in a patch and belonged to BI-RADS category 3 (arrow). FFDM, full-field digital mammography; BI-RADS, breast imaging reporting and data system.

gland overlap, primary breast lesions (breast inflammation, primary breast tumors, sclerosing adenopathy, radioactive scars, etc.) and secondary changes of breast (postoperative scars, trauma, etc.). About 1/2 to 2/3 of the primary architectural distortion is malignant. However, FFDM is limited by the spatial resolution and contrast. It is difficult to differentiate the architectural distortion and dense glands. Besides, some architectural distortions are negative in ultrasound examination, therefore ultrasound is not preferred in the assessment of architectural distortion. The diagnostic value of breast MRI for the architectural distortion is higher than FFDM. Therefore, MRI should be performed when the architectural distortion was detected in FFDM.

The diagnostic value of FFDM for architectural distortion

Local architectural distortion is a common sign of breast cancer on FFDM that can exist at the same time as asymmetric density. For non-mass breast diseases on mammography, under many circumstances, local architectural distortion is the only positive sign for the diagnosis of breast disease. Although the probability of malignancy of BI-RADS category 2 lesions is less than 2%, mammographic examination of this type of patient may lead to misdiagnosis or missed diagnosis (5). Our study found that among this type of lesion, the malignancy of local architectural distortions combined or not with asymmetric density did not differ substantially, both malignancy rates being <40%. The positive predictive values of local architectural distortion, asymmetric density, and local architectural distortion plus asymmetric density were 17.05% (15/88), 42.53% (37/87), and 36.36% (16/44), respectively. Rangayyan *et al.* (6) have shown that half to two-thirds of breast primary local architectural distortion lesions are malignant. However, it is difficult for mammography to distinguish patients with local architectural distortion from patients with asymmetric density due to its limited spatial resolution and contrast (7). Additionally, some architectural distortions are negative on ultrasound examination, so some benign lesions undergo unnecessary biopsy or surgery, and some malignant lesions are missed, leading to delayed treatment and poorer prognosis. Our study also showed that the diagnostic specificity of FFDM for local architectural distortion lesions was 41.7%, which is close to the diagnostic specificity of FFDM for breast cancer (39.7%) reported by Schueller *et al.* (8). Some scholars believe that architectural distortions have high positive predictive values and should be biopsied (9,10). Therefore, we targeted architectural distortions of BI-RADS category 3–4 by mammography, and our results showed that the positive predictive value of BI-RADS category 3 lesions as diagnosed by mammography was only 15.3% (11/72) suggesting that mammography is not reliable for the follow-up or health management of BI-RADS category 3 lesions.

Table 5 BI-RADS classifications of the local architectural distortion according to different methods

Examinations	Lesions	BI-RADS 1–2			BI-RADS 3			BI-RADS 4			BI-RADS 5		
		Lesions	Benign	Malignant	Lesions	Benign	Malignant	Lesions	Benign	Malignant	Lesions	Benign	Malignant
FFDM	219	0*	0	0	72*	62	10	147*	90	57	0*	0	0
FFDM + DCE-MRI	219	0*	0	0	132*	124	8	71*	27	44	16*	0	16
FFDM + DCE-MRI + ADC	219	59*	59	0	87*	85	2	39*	4	35	34*	0	34

*, for sum of benign and malignant lesions in the same BI-RADS category. BI-RADS, breast imaging reporting and data system; FFDM, full-field digital mammography; DCE-MRI, dynamic contrast-enhanced MRI.

The diagnostic efficiency of MRI for BI-RADS category 3 architectural distortions on mammography

DCE-MRI combined with DWI has high sensitivity and specificity for the diagnosis of breast cancer, but the diagnostic value of MRI for architectural distortions seen on mammography is not clear (11,12). Our study showed that architectural distortions were manifested as dot-like enhancements, mass-like enhancements, non-mass-like enhancements, and no enhancements, among which the seven cases with no enhancements and 26 cases with spot-like enhancements were benign lesions. We found that the DCE-MRI enhancement types and TIC types differed significantly between breast benign and malignant lesions, which is consistent with previous studies. Additionally, DWI had a high diagnostic efficiency in differentiating breast benign *vs.* malignant lesions, and the diagnostic threshold of the ADC value was 1.1×10^{-3} to 1.6×10^{-3} mm^2/s (13-15). We found that the sensitivity and specificity were 79.8% and 95.6%, respectively, when differentiating benign and malignant lesions with the ADC value of 1.02×10^{-3} mm^2/s, which is consistent with previous studies. The sensitivity of DCE-MRI combined with ADC in diagnosing breast benign and malignant lesions was higher than that of DCE-MRI alone. Our study showed that the specificity of DCE-MRI + ADC in differentiating breast benign *vs.* malignant lesions was higher than that of DCE-MRI + FFDM, which is consistent with the study by Ei Khouli *et al.* (16).

Among the patients diagnosed with breast tumors that were BI-RADS category 3 lesions by mammography in our study, 14 lesions were classified into MRI BI-RADS categories 4–5, and the diagnostic efficiency was significantly increased by adding MRI. The sensitivity and specificity were increased from 86.3% and 41.7% to 98.1% and 97.5%, respectively. One patient was false negative since she had mucinous adenocarcinoma mainly composed of mucus. Because a simple mucinous carcinoma is rich in mucus matrix, the ADC value is high. Pathologically, simple mucinous adenocarcinomas contain a large amount of extracellular mucus and relatively few tumor cells, so MRI enhancement of them is not significant, and it is difficult to distinguish them from simple cysts. Another patient had ductal carcinoma *in situ* with a small lesion that was not clear under the significant background parenchymal enhancement. Additionally, due to the poor spatial resolution of ADC, the ADC value was high as a result of the volume effect, which is consistent with the results by

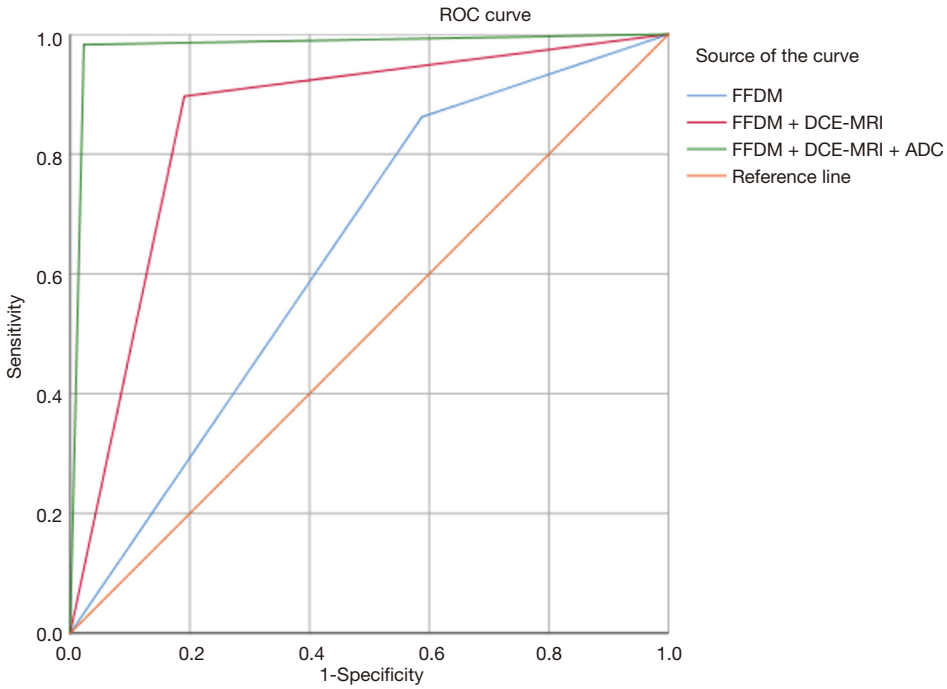

Figure 3 The AUCs of FFDM, FFDM + DCE-MRI, and FFDM + DCE-MRI + ADC in differentiating breast benign *vs.* malignant tumors were 0.647, 0.851, and 0.983, respectively. FFDM, full-field digital mammography; DCE-MRI, dynamic contrast-enhanced MRI; ADC, apparent diffusion coefficient.

Brnic *et al.* (17).

Limitations of MRI for the diagnosis of architectural distortion lesions

Although the specificity MRI for the diagnosis of architectural distortions was high, we found five false-positive and two false-negative lesions, suggesting that MRI examination has some limitations. On one hand, the diagnostic value of ADC for non-mass-like lesions is lower than that of mass-like lesions (18,19). On the other hand, there are overlaps between the differentiation thresholds of benign and malignant lesions, which we believe is related to the architectural characteristics and pathological types. Our analysis shows the following. (I) After dynamic enhancement, the enhanced breast parenchymal background will interfere with the exposure of the small lesions. Due to the limited spatial resolution, DWI usually does not show lesions smaller than 1 cm well. (II) The success of DWI is related to the pathological type of the local architectural distortion. For example, the lesions of ductal carcinomas *in situ* are restricted to the duct and do not infiltrate the surrounding normal glandular tissue. The movement of water molecules is not significantly restricted. As a result, the ADC value of the ductal carcinomas *in situ* is higher than that of the invasive ductal carcinoma. (III) Intraductal papilloma is caused by proliferation of the ductal epithelial and muscular epithelial cells, which cover the axis of the fibrous vascular bundle. The cells are aligned tightly, with a small extracellular space, so the movement of water molecules is restricted, and the ADC value is reduced. Additionally, the blood supply to the intraductal papilloma is abundant, which may be manifested as an outflow curve. As a result, the intraductal papilloma is often misdiagnosed as being malignant. (IV) The ADC values are low for some special breast lesions (such as sclerosing adenopathy) because the large number of dense fibrous tissue limits the diffusion of water molecules. (V) Mucinous adenocarcinoma is sometimes misdiagnosed as being benign due to its large amount of mucinous tissue, which leads to a loosened structure and a high ADC value. (VI) The structure of non-mass-like lesions is more scattered than that of the mass-like

lesions. There may be normal breast fibrous gland tissues inside the non-mass-like lesions, and some lesions may be small in volume, so that the measurement of ADC value is greatly impacted by the volume effect.

Limitations of this study

(I) This is a retrospective study, and we did not compare our results with ultrasonic examination. (II) FFDM is very sensitive to breast calcification, and we did not perform in-depth analysis of calcified lesions. (III) According to the 2013 BI-RADS, the lesions in category 4 by MRI are classified into three types, including types A, B, and C. There may be factors that are not accurate enough in the comparison of diagnostic efficiency. (IV) There was some bias in the patients recruited, with asymmetric dense lesions significantly more common than architectural distortions. With the progression of artificial intelligence technology and medical imaging-assisted diagnosis technology, their combination will generate novel radiomics methods that will be gradually applied to breast research. Further studies on the diagnostic efficiency of FFDM and MRI radiomics will be carried out in the future.

Conclusions

In summary, MRI can improve the diagnostic efficiency of mammography in detecting BI-RADS category 3–4 architectural distortion. MRI should be added when the architectural distortion was detected in FFDM. Patients should be followed up regularly if no significant malignant signs are detected on MRI to reduce unnecessary biopsies of benign locoregional distortion lesions and reduce missed diagnoses of malignant lesions.

Acknowledgments

Funding: None.

Footnote

Reporting Checklist: The authors have completed the STROBE reporting checklist. Available at http://dx.doi.org/10.21037/gs-20-505

Data Sharing Statement: Available at http://dx.doi.org/10.21037/gs-20-505

Conflicts of Interest: All authors have completed the ICMJE uniform disclosure form (available at http://dx.doi.org/10.21037/gs-20-505). The authors have no conflicts of interest to declare.

Ethical Statement: The authors are accountable for all aspects of the work in ensuring that questions related to the accuracy or integrity of any part of the work are appropriately investigated and resolved. This study was approved by the Ethics Committee of Ningbo Women & Children's Hospital (Approval No: EC2020-023). The trial was conducted in accordance with the Declaration of Helsinki (as revised in 2013). Written informed consent was obtained from all patients.

References

1. Liberman L, Menell JH. Breast imaging reporting and data system (BI-RADS). Radiol Clin North Am 2002;40:409-30, v.
2. Chopier J, Roedlich MN, Mathelin C. Breast imaging of mass, architectural distortion and asymmetry: Clinical practice guidelines. J Gynecol Obstet Biol Reprod (Paris) 2015;44:947-59.
3. Durand MA, Wang S, Hooley RJ, et al. Tomosynthesis-detected Architectural Distortion: Management Algorithm with Radiologic-Pathologic Correlation. Radiographics 2016;36:311-21.
4. Raichand S, Dunn AG, Ong MS, et al. Conclusions in systematic reviews of mammography for breast cancer screening and associations with review design and author characteristics. Syst Rev 2017;6:105.
5. Shaheen R, Schimmelpenninck CA, Stoddart L, et al. Spectrum of diseases presenting as architectural distortion on mammography: multimodality radiologic imaging with pathologic correlation.Semin Ultrasound CT MR 2011;32:351-62.
6. Rangayyan RM, Banik S, Desautels JE. Computer - aided

detection of architectural distortion in prior mammograms of interval cancer. J Digit Imaging 2010;23:611-31.
7. Boyer B, Russ E. Anatomical-radiological correlations: architectural distortions. Diagn Interv Imaging 2014;95:134-40.
8. Schueller G, Riedl CC, Mallek R, et al. Image quality, lesion detection, and diagnostic efficacy in digital mammography: full-field digital mammography versus computed radiography-based mammography using digital storage phosphor plates. Eur J Radiol 2008;67:487-96.
9. Mendez A, Cabanillas F, Echenique M, et al. Mammographic features and correlation with biopsy findings using 11-gauge stereotactic vacuum-assisted breast biopsy (SVABB). Ann Oncol 2004;15:450-4.
10. Pijnappel RM, Peeters PH, Hendriks JH, et al. Reproducibility of mammographic classifications for non-palpable suspect lesions with microcalcifications. Br J Radiol 2004;77:312-4.
11. Partridge SC, Rahbar H, Murthy R, et al. Improved diagnostic accuracy of breast MRI through combined apparent diffusion coefficients and dynamic contrast-enhanced kinetics. Magn Reson Med 2011;65:1759-67.
12. Kul S, Cansu A, Alhan E, et al. Contribution of diffusion-weighted imaging to dynamic contrast-enhanced MRI in the characterization of breast tumors. AJR Am J Roentgenol 2011;196:210-7.
13. Stadlbauer A, Bernt R, Gruber S, et al. Diffusion - weighted MR imaging with background body signal suppression (DWIBS) for the diagnosis of malignant and benign breast lesions. Eur Radiol 2009;19:2349-56.
14. Lo GG, Ai V, Chan JK, et al. Diffusion-weighted magnetic resonance imaging of breast lesions: first experiences at 3 T. J Comput Assist Tomogr 2009;33:63-9.
15. Yili Z, Xiaoyan H, Hongwen D, et al. The value of diffusion-weighted imaging in assessing the ADC changes of tissues adjacent to breast carcinoma. BMC Cancer 2009;9:18.
16. Ei Khouli RH, Jacobs MA, Mezban SD, et al. Diffusion-weighted imaging improves the diagnostic accuracy of conventional 3.0T breast MR imaging. Radiology 2010;256:64-73.
17. Brnic D, Brnic D, Simundic I, et al. MRI and comparison mammography: a worthy diagnostic alliance for breast microcalcifications. Acta Radiol 2016;57:413-21.
18. Ong E. Preoperative imaging for breast conservation surgery—do we need more than conventional imaging for local disease assessment? Gland Surg 2018;7:554-9.
19. Pereira FP, Martins G, Figueiredo E, et al. Assessment of breast lesions with diffusion-weighted MRI: comparing the use of different b values. AJR Am J Roentgenol 2009;193:1030-5.

Cite this article as: Mei H, Xu J, Yao G, Wang Y. The diagnostic value of MRI for architectural distortion categorized as BI-RADS category 3–4 by mammography. Gland Surg 2020;9(4):1008-1018. doi: 10.21037/gs-20-505